HHS Public Access

Author manuscript

J Magn Reson Imaging. Author manuscript; available in PMC 2019 October 01.

Published in final edited form as:

J Magn Reson Imaging. 2018 October ; 48(4): 1046–1058. doi:10.1002/jmri.26029.

Using Multidimensional Topological Data Analysis to Identify Traits of Hip OA

Jasmine Rossi-deVries, BA[1], **Valentina Pedoia, PhD**[1,+], **Michael A. Samaan, PhD**[1,3], **Adam R. Ferguson, PhD**[2,4], **Richard B. Souza, PT PhD**[1,3], and **Sharmila Majumdar, PhD**[1]

[1]Department of Radiology and Biomedical Imaging, University of California, San Francisco

[2]Weill Institute for Neurosciences, Department of Neurological Surgery, Brain and Spinal Injury Center, University of California, San Francisco

[3]Department of Physical Therapy and Rehabilitation Science, University of California, San Francisco

[4]San Francisco Veterans Affairs Medical Center, San Francisco

Abstract

BACKGROUND—Osteoarthritis (OA) is a multifaceted disease with many variables affecting diagnosis and progression. Topological Data Analysis (TDA) is a state of the art big data analytics tool that can combine all variables into multidimensional space. TDA is used to simultaneously analyze imaging and gait analysis techniques.

PURPOSE—To identify biochemical and biomechanical biomarkers able to classify different disease progression phenotypes in subjects with and without radiographic signs of hip OA.

STUDY TYPE—Longitudinal study for comparison of progressive and non progressive subjects.

POPULATION—102 subjects with and without radiographic signs of hip osteoarthritis.

FIELD STRENGTH/SEQUENCE—3T, SPGR 3D MAPSS $T_{1\rho}/T_2$, intermediate-weighted fat-suppressed fast spin-echo (FSE)

ASSESSMENT—Multidimensional data analysis including cartilage composition, bone shape, Kellgren-Laurence (KL) classification of osteoarthritis, Scoring Hip Osteoarthritis with MRI (SHOMRI), Hip disability and Osteoarthritis Outcome Score (HOOS)

STATISTICAL TESTS—Analysis done using Topological Data Analysis (TDA), Kolmogorov-Smirnov (KS) testing and Benjamini-Hochberg to rank P-value results to correct for multiple comparisons.

RESULTS—Subjects in the later stages of the disease had an increased SHOMRI score ($p < 0.0001$), increased KL ($p = 0.0012$), and older age ($p < 0.0001$). Subjects in the healthier group showed intact cartilage and less pain. Subjects found in between these two groups had a range of symptoms. Analysis of this sub-group identified knee biomechanics ($p < 0.0001$) as an initial

[+]Co-corresponding Author Contact Details: Valentia Pedoia, Phone: 1 (415) 549-46136, Valentina.Pedoia@ucsf.edu, Address: 1700 Fourth Street, Suite 201, QB3 Building San Francisco, CA, 94107.

marker of the disease that is noticeable before the morphological progression and degeneration. Further analysis of an OA sub-group with femoroacetabular impingement (FAI) showed Anterior Labral tears to be the most significant marker ($p = 0.0017$) between those FAI subjects with and without OA symptoms.

DATA CONCLUSION—The data-driven analysis obtained with TDA proposes new phenotypes of these subjects that partially overlap with the radiographic based classical disease status classification and also shows the potential for further examination of an early onset biomechanical intervention.

Keywords

cartilage; osteoarthritis; hip OA; topological data analysis; big data

INTRODUCTION

Osteoarthritis (OA) is a leading joint disorder in America(1). Over 26 million adults in the US are affected by OA which can commonly lead to disability, surgery, and hip replacement(1). OA is complex and multifactorial; both systemic and local variables have a role in the progression of the disease. Radiographic and morphological evidence has been used in the past to diagnose hip OA, however these methods are not able to detect the earlier stages of the disease. Previous studies have shown the ability of compositional imaging, $T_{1\rho}$ and T_2 cartilage mapping, to detect the structural properties and early degeneration of cartilage(2, 3). Chemical exchange in proteoglycan and water protons was suggested to contribute to $T_{1\rho}$ in cartilage, although $T_{1\rho}$ changes in cartilage may be affected by hydration and collagen structure as well(4). T_2 relaxation times are primarily affected by hydration and collagen structure due to dipolar interactions(5).

Kinematics and kinetics of both the hip and the knee are also important for the clinical assessment of OA. Previous studies have shown that loading of the knee joint is related to the progression of knee OA(6-8), but it has not yet been examined with multidimensional factors for the hip. Furthermore, hip OA pathogenesis and progression is also characterized by changes in the subchondral and trabecular bone including early-stage increased bone remodeling and bone loss, as well as, the late-stage reduced bone remodeling and subchondral densification(9, 10).

Given the multifactorial nature of OA, it might be useful to analyze all factors (i.e. morphological, compositional, and biomechanical) simultaneously. In this study, we used multidimensional data analysis to generate an OA prediction hypothesis built on the following variables: morphological and compositional cartilage assessments, gait kinematics and kinetics, and bone shape analysis.

Recent advancements in big data analytics and machine learning provide several multidimensional visualization methods with which we can compare individual patients as a ‘point-cloud’ in multidimensional space, overcoming the inherent limitations of single endpoints(11). Our approach uses the shape, or topology, of our data(11); topology is a branch of applied mathematics aimed at formally analyzing geometric shapes. Topological

Data Analysis (TDA) takes a geometric approach to pattern recognition within data. TDA extracts patterns from a multi-dimensional data set that can determine relevant sub-groups as well as present new insights about the data(11). TDA has shown promising results in several varied applications, including exploring stem cell transplant complications(12), phenotyping attention-deficit/hyperactivity disorder(13), analyzing FDA drug-target interactions(14), and a preclinical study in spinal and traumatic brain injury(15). Recently the first application of TDA to study Knee OA was presented(2) showing the usage of the technique as a descriptive tool able to identify subject sub populations and key imaging biomarkers able to predict disease progression.

We aim to use state of the art big data analytics, imaging and gait analysis techniques to simultaneously analyze all the combined variables in multidimensional space in order to assist the identification of biochemical and biomechanical biomarkers able to classify different disease progression phenotypes in subjects with and without radiographic signs of hip OA. We hypothesized that the simultaneous analysis of all the variables, in the context of a completely data-driven approach, will allow us to discover new interactions between different aspects of the disease, helping to explain the complex mechanism of hip OA pathogenesis and progression.

THEORY AND METHODS

Subjects

The subjects included in the analysis are part of a case-control study aimed to study the longitudinal changes in cartilage, biochemical composition, using magnetic resonance imaging (MRI), in subjects with and without radiographic hip OA. A total of 102 subjects were recruited. The inclusion criteria for OA patients (n=34) included definite radiographic evidence of hip OA (Kellgren-Lawrence(16) [KL>1]), while controls were classified as those subjects (n=68) without radiographic evidence of OA [KL<2]). Patients were excluded if they were involved in concurrent use of an investigational drug, had a history of fracture or surgical intervention on the studied hip, or had contradictions to MRI.

Demographic information including age, gender, body mass index (BMI), and race were collected at the time of recruitment (age: 44.0±13.7 years, BMI: 23.8±3.0 kg/m^2, 58 males (56%), 72 Caucasians (69%)). Study subjects were brought in for an MR-exam and gait analysis at baseline, 18 months and 36 months follow-up. The Hip Disability and Osteoarthritis Outcomes Score (HOOS) (17) was used to assess hip joint pain, symptoms, stiffness, function and quality of life and used a scale of 0 to 100 to indicate severe or no clinical symptoms, respectively. Evaluation of radiographs were performed using the KL grading(16) assigned by a musculoskeletal radiologist with 20 years of experience (TL). All examiners involved in grading, including KL, SHOMRI, and biomechanical examination were blinded to others' results.

MR Imaging and Image Processing

Unilateral hip MR images were acquired with a 3 Tesla MR-scanner (GE MR750; GE Healthcare, Waukesha, WI) using an 8-channel receive-only coil (GE Healthcare, Waukesha,

WI). MRI protocol and sequences are described by Gallo et al(18). The MRI protocol included intermediate-weighted fat-suppressed fast spin-echo (FSE) sequences in the sagittal, oblique coronal, and oblique axial orientations described in Wyatt et. al (3). These sequences were used for semi-quantitative clinical grading of hip joint abnormalities using the Scoring Hip Osteoarthritis with MRI (SHOMRI) scoring system which provides 52 morphological variables described in detail in Lee et al (19, 20). A combined $T1_\rho/T_2$ mapping sequence using a 3D segmented SPGR acquisition was used to assess cartilage proteoglycan content($T1_\rho$) and collagen orientation(T_2), where an increase in $T1_\rho$ and T_2 relaxation times indicated reduced proteoglycan content and altered collagen structure, respectively(21). All image processing was performed using an in-house program developed in MATLAB (The Mathworks, Na tick, MA)(22). Femoral and acetabular cartilage compartment segmentation was done with an edge-based, semi-automatic method previously described and evaluated(3), to obtain $T_{1\rho}$ and T_2 relaxation times in various subregions as described in Pedoia et al (23-25).

The proximal femur bone of all the subjects were segmented automatically on the T_{1p}-weighted image with TSL = 0 using an atlas-based method refined by active contours. All the segmentations underwent a strict protocol of quality control and a single user that manually adjusted the bone segmentation in case of failure of the automatic procedure. Bone shape analysis was performed using 3D-statistical shape modeling as previously described and evaluated(26), where 20 modes of variation describing the 3D shape of the proximal femur were extracted and considered for the analysis.

Kinematics and Kinetics

Biomechanical data acquisition used in this study is similar to previous work(27) and is briefly described below. A 10-camera motion capture system (VICON, Oxford Metrics, Oxford, UK) was used to obtain 3D position data at a sampling rate of 250 Hz, while ground reaction forces (GRF) were obtained simultaneously using two embedded force platforms (AMTI, Watertown, MA, USA) at a sampling rate of 1000 Hz. Forty-one retroflective markers were placed at anatomical landmarks and used to track segment position, while subjects walked at a fixed speed (1.35m/s) (27). The Visual3D (C-Motion, Germantown, MD) software was used to calculate lower extremity joint kinematics and moments by using an unweighted least squares method(28) and inverse dynamics, respectively. Joint angels were normalized to a static calibration trial obtained prior to the gait trials. External hip and knee joint moments were normalized by body mass and height (Nm/kg*m). Joint moment impulses were computed as the integral of the moment with respect to time (Nm*ms/kg*m). GRF data was normalized by body weight (BW). GRF, hip and knee joint kinematic and kinetic variables (Supplementary Table 1) were computed for each subject during four successful gait trials, as described in Samaan et al (23) and were used to obtain the subject's average measures which were used for analysis.

Multi-Dimensional Data

From our processing pipeline we obtain a description for each patient consisting of 181 variables including: demographics (8 variables), PROMs (Patient Reported Outcome Measures) (29 variables), X-rays (1 variable), morphological MRI (52 variables),

compositional MRI (26 variables), gait kinematics and kinetics (42 variables), and bone shape analysis (20 variables). Supplementary Table 1 includes a data dictionary of all variables. All baseline data was used to build the topological shape, but the progression variables were built from baseline, 18 month and 36 month data. Three progression variables (two compositional progression and one clinical HOOS pain progression) were added in order to examine change over time in compositional $T_{1\rho}$ and T_2 variables as well as HOOS pain change over time (Table 1):

Compositional Progression Definition (Femoral and Acetabular)—Subjects who showed no cartilage lesion progression over three years (ΔSHOMRI total cartilage grade = 0) and had a KL grade of <2 (n = 27) were considered to be the stable reference control cohort. This cohort was used to study the distribution of both $T_{1\rho}$ and T_2 changes over time unrelated with disease progression but reflecting technical repeatability and normal aging of the study population. The average (AVG_{norm}) and standard deviation (SD_{norm}) of the longitudinal changes (3 Year-Baseline) within the reference control cohort were computed for each of the acetabular and femoral cartilage subcompartments. Subjects with longitudinal $T_{1\rho}$ and T_2 changes (3 Year-Baseline) in any of the cartilage sub compartment values that were within $AVG_{norm}+2*SD_{norm}$ were considered part of the "compositional non progression" cohort. All remaining subjects with longitudinal $T_{1\rho}$ and T_2 changes (3 Year-Baseline) that exceeded the $AVG_{norm}\_2*SD_{norm}$ within any of the cartilage sub compartment values were considered part of the "compositional progression" cohort. Study subjects with $T_{1\rho}/T_2$ femoral cartilage progression (n=28) and $T_{1\rho}/T_2$ acetabular cartilage progression (n=27) were separated for analysis.

Clinical HOOS Pain Progression Definition—Changes in HOOS pain, symptoms, stiffness, function, and quality of life score over the three year period (3 Year – Baseline) were computed. Subjects that exhibited a decrease of >10, indicating a worsening of HOOS related sub-scores, in any of the 5 HOOS sub-scales were considered part of the "symptomatic progression" cohort (n = 19).

Topological Data Analysis

The Topological Data Analysis (TDA) method involves mapping each patient as a multidimensional point into the "OA syndromic space" as described in Pedoia et al (2). TDA is a data driven tool that allows researchers to project all variables simultaneously into an interconnected network, in order to derive a hypothesis from the generated network shape.

The data analysis was performed using Ayasdi cloud-based platform (Ayasdi, Inc.v.3.0). The TDA network was built by integrating the multi-dimensional data described above, such as MRI morphological grading, MRI compositional analysis, biomechanical data, and bone shape analysis. The workflow automatically renders cross correlations across all selected variables and places individuals into a multidimensional point cloud space viewed through a mathematical 'lens' used for dimensionality reduction. The extracted network was built on two lenses of Metric principal component analysis (PCA) (resolution = 30, gain = 5) and a third lens of Total Cartilage Score (resolution = 12, gain = 5).

TDA iteratively clusters subjects based on their similarity where similar individuals were grouped into nodes. At each iteration, the clusters are randomly defined in terms of shape and level of overlap. The topological net is the results of the combination of all the iterations resulting in robustness of the technique.

Further details about the TDA pipeline and theory are reported in Lum et al (11). The mapping of subjects based on the selected variables into this hip OA network is referred to as the hip OA syndromic space. The results of TDA is a network in which each 'node' represents a cluster of subjects that share similar patterns between quantitative variables used to build the network. A single subject can fall in two or more clusters at different iterations of the algorithm, in which case the two nodes are connected by an 'edge'. By iterating this process, we obtain a network in which the length of the path along the edges between two nodes represents the similarity of the subjects included in the nodes. Figure 1 shows an example of the specific TDA network that we obtained; this network is color coded for number of subjects per node.

The two phases of TDA are 1) **hypothesis generation**: which includes visual inspection of the color-coded network and identification of subpopulations within the network and 2) **hypothesis evaluation**: which includes formal statistical Kolmogorov-Smirnov (KS) testing and regression to evaluate the validity of the subpopulations identified in the first phase. The Benjamini-Hochberg method is used to rank the P-value results from the KS test; this will correct for multiple comparisons.

RESULTS

The topology extracted from the data, including morphological, compositional, biomechanical, and shape analysis, produced a network with a clear separation between subjects with radiographic OA (red nodes) in the upper region and subjects without OA (blue nodes) in the lower right; this is an indication of network validity when analyzing OA (Figure 2). Based on visual assessment of Figure 2 there is a relationship between subnetwork1 and the presence of radiographic signs of hip OA. Of the 102 subjects analyzed, 34 showed radiographic signs of osteoarthritis (KL > 1) with an average age of 51.31±13.40 compared to the 68 subjects without radiographic OA (KL < 2) with an average age of 40.98±12.30. KS testing was performed on subjects in subnetwork1 (n=32) and we observed age 53.1±11.8 years (p=2.77E-07) and cartilage score 7.6±4.6 (p=4.09E-10) to be the top predictors of membership into subnetwork1 compared to the rest of the network (age: 39.8±12.4 years, Cartilage Score: 1.4±1.7) which was significantly lower in both age and cartilage lesion scores. The results of the KS test, Table 2a, shows the top statistically significant variables between subnetwork1 and the remaining subjects. (Full list of ranked variables found in Supplementary Table 2a). Morphological variables (Figure 2b) were able to separate subnetwork1 from the rest of the network, but were unable to differentiate between the wider KL range in Figure 2a.

Progression color-coded networks for hip joint pain and $T_{1\rho}/T_2$ Acetabular and Femoral compositional progression were computed using longitudinal data in order to investigate the effects over time compared to all the baseline variables used to build the network. Average

and standard deviation of the reference groups for each cartilage subcompartment as described in Gallo et al (15):

(Femoral $T_{1\rho}$ subcompartments: 2 = −0.61±4.4, 3 = −0.29±4.1, 4 = 1.12±3.5, 5 = 0.94±2.3, 6 = 0.31±2.3, 7 = −0.05±3.5),

(Femoral T_2 subcompartments: 2 = −0.08±4.1, 3 = 0.18±3.5, 4 = 1.22±3.0, 5 = 0.77±2.9, 6 = 0.19±2.9, 7 = 0.03±3.1),

(Acetabular $T_{1\rho}$ subcompartments: 2 = 0.39±3.1, 3 = 0.89±3.7, 4 = 0.11±3.3, 5 = −0.52±2.4, 6 = 1.18±3.4),

(Acetabular T_2 subcompartments: 2 = 0.68±4.4, 3 = 1.58±5.0, 4 = 1.27±3.6, 5 = 1.16±3.6, 6 = (not enough data))

$T_{1\rho}/T_2$ Femoral progression (n = 28) and $T_{1\rho}/T_2$ Acetabular progression (n = 27) were separated. “Symptomatic progression” cohort (decrease in HOOS pain <10) was instead made by 19 subjects. Table 1 reports demographics of all the subgroups.

Upon analysis of the progression colored networks (Figure 3) the upper portion contains subjects with both pain and $T_{1\rho}/T_2$ progression which is consistent with our previous findings of subnetwork1 being the portion of the cohort with more severe radiographic evidence of hip OA. The lower right of the progression colored networks in Figure 3 show a relationship with healthy controls with low pain progression and low $T_{1\rho}/T_2$ progression (shown in blue). Further visual assessment shows an inverse relationship between pain progression and compositional progression in subnetwork2 which is inconsistent with the remaining subjects shown in Figure 4:

Subnetwork 2a: Age: 46.8 ±13.8 years, (7 Female, BMI: 23.3±3.0) No $T_{1\rho}/T_2$ Progression: n=34 (59.65%), HOOS Pain Progression: n=12 (21.05%)

Subnetwork 2b: Age: 43.8 ±12.8 years, (11 Female, BMI: 23.4±3.7) $T_{1\rho}/T_2$ Progression: n=23 (40.35%), No Pain Progression: n=45 (78.95%)

The simultaneous analysis of compositional and symptomatic progression performed by TDA suggested different grouping characterized by an inverse relationship between symptomatic and compositional progression: subnetworks 1 and 3, that include subjects at the edge of disease spectrum, radiographic hip OA controls and subjects with clear signs of hip OA for which TDA analysis suggest a direct relationship between increase in symptoms and cartilage degeneration; and subnetwork2 for which this relationship appeared inverted, subjects that progress in cartilage degeneration show a regression in symptoms and vice versa. This hypothesis was verified by stratifying the patients based on the subnetwork memberships and testing direct Pearson correlations between compositional MRI and HOOS pain longitudinal variation. Both tests resulted in one statistically significant global pattern and the other approaching significance and, as hypothesized using TDA, showing inverse R-value: subnetwork 1 and 3 relationship between 3 Year pain and global delta $T_{1\rho}$ (R-value = −0.64, p-value = 0.0005) and T_2 (R-value = −0.36, p-value = 0.07); subnetwork 2 $T_{1\rho}$ (R-value = 0.28, p-value = 0.076) and T_2 (R-value = 0.35, p-value = 0.019).

As a second step, KS statistical analysis was performed to assess the main variables separating subnetwork2 and the rest of the network. Table 2b shows the top statistically significant differences between subnetwork2 and the remaining subjects; knee joint kinematics and kinetics were observed to be the top predictors for membership within subnetwork2. (Full list of ranked variables found in Supplementary Table 2b). Subjects within subnetwork2 exhibited a reduced peak knee flexion angle −16.63 ±4.1° (p=0.000485) and first peak knee flexion moment −0.49±0.2 Nm/kg*m (p=4.91E-08) compared to the rest of the subjects (−21.27±4.2°, −0.72±0.2 Nm/kg*m). Biomechanical variables were able to separate subnetwork2 from the rest of the network, but unable to separate subnetwork1 (OA group) from the rest of the network or differentiate between the healthy controls and the rest of the network.

Upon examination of Table 2a and Table 2b, it is important to mention that while this is a long list of significant variables, some of the variables are strongly correlated with each other. For example, in Table 2a, “TotalCartilageScore” is a SHOMRI variable made up of all the SHOMRI “Cartilage Lesion” scores combined; in this way, each “CartilageLesion” variable in Table 2a makes up a portion of the TotalCartilageScore. These variables could potentially be reduced to simple, TotalCartilageScore, SHOMRI_Total, age, KneeKinetics_ExMImp2, and KL. Similarly, with Table 2b, all significant variables listed can be narrowed to Flexion and Extension moment impulses, flexion and extension peak moments, SHOMRI CartilageScore, etc. Each stage of gait is connected, so it is not a surprise that a collection of similar variables is found significant.

In order to sub-classify specific OA phenotypes, patients with radiographic femoroacetabular impingement (FAI) were analyzed using this model. Once the network was color coded for group during recruitment, those FAI subjects can be seen in Figure 5a within the yellow nodes. This figure shows FAI subjects falling in both subnetwork1 (OA symptomatic group) and subnetwork3 (healthy, asymptomatic group). Statistical analysis and TTest was done on the FAI subjects within these two subgroups to see what separated these two distinct subnetworks. The variable separating the groups with the lowest P-value (0.0017) was SHOMRI Labrum Oblique Axial in the Anterior Labrum(AL) followed by SHOMRI Total (p=0.005) and then Hoos Pain Score (p=0.006). Upon examination of the TDA model, color coded for SHOMRI scored labral damage, the separation is visibly noticeable. Total Labrum Score (Figure 5b) and specifically Anterior Labrum Score (Figure 5c) shows a similar coloring with that of the radiographic KL separation (Figure 2a). The other SHOMRI scoring for Labrum, the posterior and anterior superior, were not significant.

DISCUSSION

It is necessary to characterize particular OA traits or phenotypes from available data in order to classify and diagnose patients. A common approach in the past has been to use single-variable analysis in order to classify traits or phenotypes of OA. TDA overcomes these single-variable limitations by allowing for a multidimensional analysis of all available data simultaneously. The TDA tool allows for visualization of every subpopulation within a dataset which leads to novel hypothesis generation otherwise unavailable if done with single-variable investigation.

Previous studies have looked at the association between $T_{1\rho}$ and T_2 relaxation times and presence of cartilage lesions and found that compositional MRI data could be a potential biomarker for OA(18, 29). In addition, further studies have correlated acetabular cartilage defects with higher patient reported pain(30). We could expect, therefore, to see a pattern of OA disease progression which includes increased $T_{1\rho}$ relaxation times, increased cartilage defects, and increase in pain outcome. However, it has yet to be proven that increased pain and increased $T_{1\rho}$ are correlated despite this suggested pattern. We would expect to see this similarity in the hip, however it was only found in two out of the three subnetworks. Within subnetwork1, subjects with characteristics suggesting disease progression, showed the expected relationship between pain and $T_{1\rho}/T_2$ values. Within subnetwork3, those subjects who were classified as non-progressors with healthy cartilage exhibited no pain or compositional progression. However, subjects within subnetwork2 increased in pain while showing no change in cartilage composition and the other half showed no change in pain while increasing compositional progression. As there was no radiographic or morphological evidence of disease progression within subnetwork2, it would be extremely difficult to diagnose these patients as potential disease progressors using standard radiographic and MR-based assessments of hip joint morphology, yet with TDA we are able to observe other factors that may play a role in disease progression within subnetwork2. Our analysis showed that the defining characteristics separating subnetwork2 from the rest of the network were knee joint mechanics.

Subjects in subnetwork2 ambulated with a more extended knee joint compared to the rest of the network and may potentially affect hip joint mechanics as well. Although we did not observe any differences in hip joint mechanics between subnetwork2 and the rest of the cohort, previous work has showed reduced peak hip extension and external hip flexion moment in (27, 31) subjects with hip OA and suggests sagittal plane hip joint mechanics may be an important factor in disease progression. Similar to the results of our study, previous work (31) has demonstrated reduced knee joint excursions in patients with hip OA. We found knee range of motion to be the most prevalent factor separating subnetwork2 from both the healthy subjects (subnetwork3) and those with strong signs of OA (subnetwork1). Because walking speed was controlled, less flexion and extension at the knee would force a shorter stride length with a higher stride rate. This change in gait may be responsible for the inversion of pain and $T_{1\rho}$ progression in subnetwork2. These altered knee joint mechanics observed in subjects within subnetwork2 may be early indicators of hip joint pain worsening or early signs of hip joint degeneration. Reduced knee range of motion, which may lead to reduced hip range of motion, could be one method used to adapt for pain in the early stages of the disease before radiographic or morphological signs are present.

The biomechanical separation in subjects within subnetwork2 suggest that knee joint mechanics may be a contributing factor in the early signs of hip joint pain progression or degeneration. Subnetwork2a and subnetwork2b both share the change in gait pattern mentioned above, but their inversion of $T_{1\rho}$ and pain progression is visibly separated by age. It is possible that knee joint mechanics in subjects within subnetwork2 may be aimed at reducing pain but this in turn may be altering the loading patterns within the hip joint, which may cause alterations in cartilage composition. On the other hand, subjects within subnetwork2 that exhibit longitudinal alterations in cartilage composition without

progression of pain may be performing tasks, such as jumping and cutting, on a more frequent basis, due to a lack of pain and thereby applying larger loads to the hip joint. Intervention programs targeted at adjusting knee joint mechanics in these subjects may help to reduce or prevent the progression of pain and/or alterations in cartilage composition. Future studies should perform longitudinal gait analyses in the subjects described within subnetwork2 in order to determine whether or not a clear change in lower extremity mechanics occurs that may help to further explain the inverse relationship between progression of hip joint pain and cartilage composition.

According to previous studies, it is well known that FAI is heavily associated with the progression of OA (32-34). The bony cam outcropping causing the impingement of FAI can result in both symptomatic and asymptomatic patients. Those patients whose FAI leads to OA commonly report symptoms of pain; whether this is a result of either the impingement, the OA, or both is essential in diagnosing as well as classifying each individual. Labral tears are also known to be commonly associated with FAI symptomatic patients (32, 33, 35). While it is not yet proven that labral tears are the cause of pain in FAI or that those subjects with labral tears might progress to OA faster or more easily than those FAI patients without labral tears, there is still some literature supporting these hypotheses (36, 37). Those subjects with greater symptoms of OA, most notably high KL scores, and greater pain also show significantly higher labral tears; further investigation is needed, however this model gives strong evidence towards the idea that labral scores are able to stratify patients similarly to pain progression as well as KL scores.

Although this data shows promising results, there are study limitations that need to be addressed. The short follow-up time and small sample size require further investigation in order to confirm the results of this study. The design of this study included various levels of osteoarthritis and a different study design could take into account this variety of disease as well as age. In addition, our results were limited by the use of longitudinal hip joint cartilage composition and pain progression analysis and the use of cross-sectional biomechanics data. A morphological progression variable was unable to be accurately predictive or useful given the short time frame and the sample size of the study. This means that particular morphological features attributed to OA might have been overlooked given the design of the study and that overall variables such as Total Cartilage Score and Total SHOMRI Score took precedent over more specific morphological scorings. In the future, the study design could be adjusted to include the ability to observe longitudinal changes in hip joint morphology.

In conclusion, by use of multidimensional TDA, we were able to map all variables simultaneously into the OA syndromic space and observe a visual separation of subnetworks. This separation is characterized by common traits leading to different stages of hip OA. We showed the importance of including all data upon diagnoses including morphological, patient reported pain, compositional, and biomechanics data and demonstrated the ability to classify different phenotypes of OA based off of multiple variables as opposed to single reference points.

Supplementary Material

Refer to Web version on PubMed Central for supplementary material.

Acknowledgments

- Conception and design: Sharmila Majumdar.
- Collection and processing of data: Jasmine Rossi-deVries, Valentina Pedoia, Michael Samaan
- Analysis and interpretation of the data: Jasmine Rossi-deVries, Valentina Pedoia, Michael Samaan, Sharmila Majumdar, Thomas Link, Alan Zhang
- Biomechanics Expertise: Richard B. Souza and Michael Samaan
- Drafting of the article: Jasmine Rossi-deVries and Valentina Pedoia
- Obtaining funding: Sharmila Majumdar and Valentina Pedoia
- Final approval of the article: All the authors

Grant Support: P50 AR060752 (SM), R01AR046905 (SM), K99AR070902 (VP)

References

1. Zhang Y, Jordan JM. Epidemiology of osteoarthritis. Clin Geriatr Med. 2010; 26(3):355–69. DOI: 10.1016/j.cger.2010.03.001 [PubMed: 20699159]
2. Pedoia V, Haefeli J, Morioka K, Teng HL, Nardo L, Souza RB, et al. MRI and biomechanics multidimensional data analysis reveals R2-R1rho as an early predictor of cartilage lesion progression in knee osteoarthritis. J Magn Reson Imaging. 2017; doi: 10.1002/jmri.25750
3. Wyatt C, Kumar D, Subburaj K, Lee S, Nardo L, Narayanan D, et al. Cartilage T1rho and T2 Relaxation Times in Patients With Mild-to-Moderate Radiographic Hip Osteoarthritis. Arthritis Rheumatol. 2015; 67(6):1548–56. DOI: 10.1002/art.39074 [PubMed: 25779656]
4. Li X, Cheng J, Lin K, Saadat E, Bolbos RI, Jobke B, et al. Quantitative MRI using T1rho and T2 in human osteoarthritic cartilage specimens: correlation with biochemical measurements and histology. Magn Reson Imaging. 2011; 29(3):324–34. DOI: 10.1016/j.mri.2010.09.004 [PubMed: 21130590]
5. Nieminen MT, Rieppo J, Toyras J, Hakumaki JM, Silvennoinen J, Hyttinen MM, et al. T2 relaxation reveals spatial collagen architecture in articular cartilage: a comparative quantitative MRI and polarized light microscopic study. Magn Reson Med. 2001; 46(3):487–93. [PubMed: 11550240]
6. Souza RB, Kumar D, Calixto N, Singh J, Schooler J, Subburaj K, et al. Response of knee cartilage T1rho and T2 relaxation times to in vivo mechanical loading in individuals with and without knee osteoarthritis. Osteoarthritis Cartilage. 2014; 22(10):1367–76. DOI: 10.1016/j.joca.2014.04.017 [PubMed: 24792208]
7. Souza RB, Baum T, Wu S, Feeley BT, Kadel N, Li X, et al. Effects of unloading on knee articular cartilage T1rho and T2 magnetic resonance imaging relaxation times: a case series. J Orthop Sports Phys Ther. 2012; 42(6):511–20. DOI: 10.2519/jospt.2012.3975 [PubMed: 22402583]
8. Calixto NE, Kumar D, Subburaj K, Singh J, Schooler J, Nardo L, et al. Zonal differences in meniscus MR relaxation times in response to in vivo static loading in knee osteoarthritis. J Orthop Res. 2016; 34(2):249–61. DOI: 10.1002/jor.23004 [PubMed: 26223430]
9. Muller-Gerbl M, Putz R, Hodapp N, Schulte E, Wimmer B. Computed tomography-osteoabsorptiometry for assessing the density distribution of subchondral bone as a measure of long-term mechanical adaptation in individual joints. Skeletal Radiol. 1989; 18(7):507–12. [PubMed: 2588028]
10. Muller-Gerbl M, Putz R, Kenn R. Demonstration of subchondral bone density patterns by three-dimensional CT osteoabsorptiometry as a noninvasive method for in vivo assessment of individual long-term stresses in joints. J Bone Miner Res. 1992; 7(Suppl 2):S411–8. DOI: 10.1002/jbmr.5650071409 [PubMed: 1485549]

11. Lum PY, Singh G, Lehman A, Ishkanov T, Vejdemo-Johansson M, Alagappan M, et al. Extracting insights from the shape of complex data using topology. Sci Rep. 2013; 3:1236.doi: 10.1038/srep01236 [PubMed: 23393618]
12. Lakshmikanth T, Olin A, Chen Y, Mikes J, Fredlund E, Remberger M, et al. Mass Cytometry and Topological Data Analysis Reveal Immune Parameters Associated with Complications after Allogeneic Stem Cell Transplantation. Cell Rep. 2017; 20(9):2238–50. DOI: 10.1016/j.celrep.2017.08.021 [PubMed: 28854371]
13. Kyeong S, Kim JJ, Kim E. Novel subgroups of attention-deficit/hyperactivity disorder identified by topological data analysis and their functional network modular organizations. PLoS One. 2017; 12(8):e0182603.doi: 10.1371/journal.pone.0182603 [PubMed: 28829775]
14. Lin HH, Zhang LL, Yan R, Lu JJ, Hu Y. Network Analysis of Drug-target Interactions: A Study on FDA-approved New Molecular Entities Between 2000 to 2015. Sci Rep. 2017; 7(1):12230.doi: 10.1038/s41598-017-12061-8 [PubMed: 28947756]
15. Nielson JL, Paquette J, Liu AW, Guandique CF, Tovar CA, Inoue T, et al. Topological data analysis for discovery in preclinical spinal cord injury and traumatic brain injury. Nat Commun. 2015; 6:8581.doi: 10.1038/ncomms9581 [PubMed: 26466022]
16. Kellgren JH, Lawrence JS. Radiological assessment of osteo-arthrosis. Ann Rheum Dis. 1957; 16(4):494–502. [PubMed: 13498604]
17. Nilsdotter AK, Lohmander LS, Klassbo M, Roos EM. Hip disability and osteoarthritis outcome score (HOOS)–validity and responsiveness in total hip replacement. BMC Musculoskelet Disord. 2003; 4:10.doi: 10.1186/1471-2474-4-10 [PubMed: 12777182]
18. Gallo MC, Wyatt C, Pedoia V, Kumar D, Lee S, Nardo L, et al. T1rho and T2 relaxation times are associated with progression of hip osteoarthritis. Osteoarthritis Cartilage. 2016; 24(8):1399–407. DOI: 10.1016/j.joca.2016.03.005 [PubMed: 26973330]
19. Lee S, Nardo L, Kumar D, Wyatt CR, Souza RB, Lynch J, et al. Scoring hip osteoarthritis with MRI (SHOMRI): A whole joint osteoarthritis evaluation system. J Magn Reson Imaging. 2015; 41(6):1549–57. DOI: 10.1002/jmri.24722 [PubMed: 25139720]
20. Schwaiger BJ, Gersing AS, Lee S, Nardo L, Samaan MA, Souza RB, et al. Longitudinal assessment of MRI in hip osteoarthritis using SHOMRI and correlation with clinical progression. Semin Arthritis Rheum. 2016; 45(6):648–55. DOI: 10.1016/j.semarthrit.2016.04.001 [PubMed: 27162009]
21. Li X, Majumdar S. Quantitative MRI of articular cartilage and its clinical applications. J Magn Reson Imaging. 2013; 38(5):991–1008. DOI: 10.1002/jmri.24313 [PubMed: 24115571]
22. Carballido-Gamio J, Bauer J, Lee KY, Krause S, Majumdar S. Combined image processing techniques for characterization of MRI cartilage of the knee. Conf Proc IEEE Eng Med Biol Soc. 2005; 3:3043–6. DOI: 10.1109/IEMBS.2005.1617116 [PubMed: 17282885]
23. Carballido-Gamio J, Bauer JS, Stahl R, Lee KY, Krause S, Link TM, et al. Inter-subject comparison of MRI knee cartilage thickness. Med Image Anal. 2008; 12(2):120–35. DOI: 10.1016/j.media.2007.08.002 [PubMed: 17923429]
24. Carballido-Gamio J, Link TM, Li X, Han ET, Krug R, Ries MD, et al. Feasibility and reproducibility of relaxometry, morphometric, and geometrical measurements of the hip joint with magnetic resonance imaging at 3T. J Magn Reson Imaging. 2008; 28(1):227–35. DOI: 10.1002/jmri.21411 [PubMed: 18581346]
25. Pedoia V, Gallo MC, Souza RB, Majumdar S. Longitudinal study using voxel-based relaxometry: Association between cartilage T1rho and T2 and patient reported outcome changes in hip osteoarthritis. J Magn Reson Imaging. 2017; 45(5):1523–33. DOI: 10.1002/jmri.25458 [PubMed: 27626787]
26. Pedoia V, Samaan MA, Inamdar G, Gallo MC, Souza RB, Majumdar S. Study of the interactions between proximal femur 3d bone shape, cartilage health, and biomechanics in patients with hip Osteoarthritis. J Orthop Res. 2017; doi: 10.1002/jor.23649
27. Samaan MA, Teng HL, Kumar D, Lee S, Link TM, Majumdar S, et al. Acetabular cartilage defects cause altered hip and knee joint coordination variability during gait. Clin Biomech (Bristol, Avon). 2015; 30(10):1202–9. DOI: 10.1016/j.clinbiomech.2015.08.003

28. Spoor CW, Veldpaus FE. Rigid body motion calculated from spatial co-ordinates of markers. J Biomech. 1980; 13(4):391–3. [PubMed: 7400168]
29. Liebl H, Joseph G, Nevitt MC, Singh N, Heilmeier U, Subburaj K, et al. Early T2 changes predict onset of radiographic knee osteoarthritis: data from the osteoarthritis initiative. Ann Rheum Dis. 2015; 74(7):1353–9. DOI: 10.1136/annrheumdis-2013-204157 [PubMed: 24615539]
30. Kumar D, Wyatt CR, Lee S, Nardo L, Link TM, Majumdar S, et al. Association of cartilage defects, and other MRI findings with pain and function in individuals with mild-moderate radiographic hip osteoarthritis and controls. Osteoarthritis Cartilage. 2013; 21(11):1685–92. DOI: 10.1016/j.joca.2013.08.009 [PubMed: 23948977]
31. Eitzen I, Fernandes L, Nordsletten L, Risberg MA. Erratum: Sagittal plane gait characteristics in hip osteoarthritis patients with mild to moderate symptoms compared to healthy controls: a cross-sectional study. BMC Musculoskelet Disord. 2015; 16:52.doi: 10.1186/s12891-015-0483-8 [PubMed: 25887966]
32. Beck M, Kalhor M, Leunig M, Ganz R. Hip morphology influences the pattern of damage to the acetabular cartilage: femoroacetabular impingement as a cause of early osteoarthritis of the hip. J Bone Joint Surg Br. 2005; 87(7):1012–8. DOI: 10.1302/0301-620X.87B7.15203 [PubMed: 15972923]
33. Anderson LA, Peters CL, Park BB, Stoddard GJ, Erickson JA, Crim JR. Acetabular cartilage delamination in femoroacetabular impingement. Risk factors and magnetic resonance imaging diagnosis. J Bone Joint Surg Am. 2009; 91(2):305–13. DOI: 10.2106/JBJS.G.01198 [PubMed: 19181974]
34. Ganz R, Leunig M, Leunig-Ganz K, Harris WH. The etiology of osteoarthritis of the hip: an integrated mechanical concept. Clin Orthop Relat Res. 2008; 466(2):264–72. DOI: 10.1007/s11999-007-0060-z [PubMed: 18196405]
35. Samaan MA, Pedoia V, Zhang AL, Gallo MC, Link TM, Souza RB, et al. A novel mr-based method for detection of cartilage delamination in femoroacetabular impingement patients. J Orthop Res. 2017; doi: 10.1002/jor.23667
36. Suarez-Ahedo C, Gui C, Rabe SM, Walsh JP, Chandrasekaran S, Domb BG. Relationship Between Age at Onset of Symptoms and Intraoperative Findings in Hip Arthroscopic Surgery. Orthop J Sports Med. 2017; 5(11) 2325967117737480. doi: 10.1177/2325967117737480
37. Kim YH. Acetabular dysplasia and osteoarthritis developed by an eversion of the acetabular labrum. Clin Orthop Relat Res. 1987; 215:289–95.

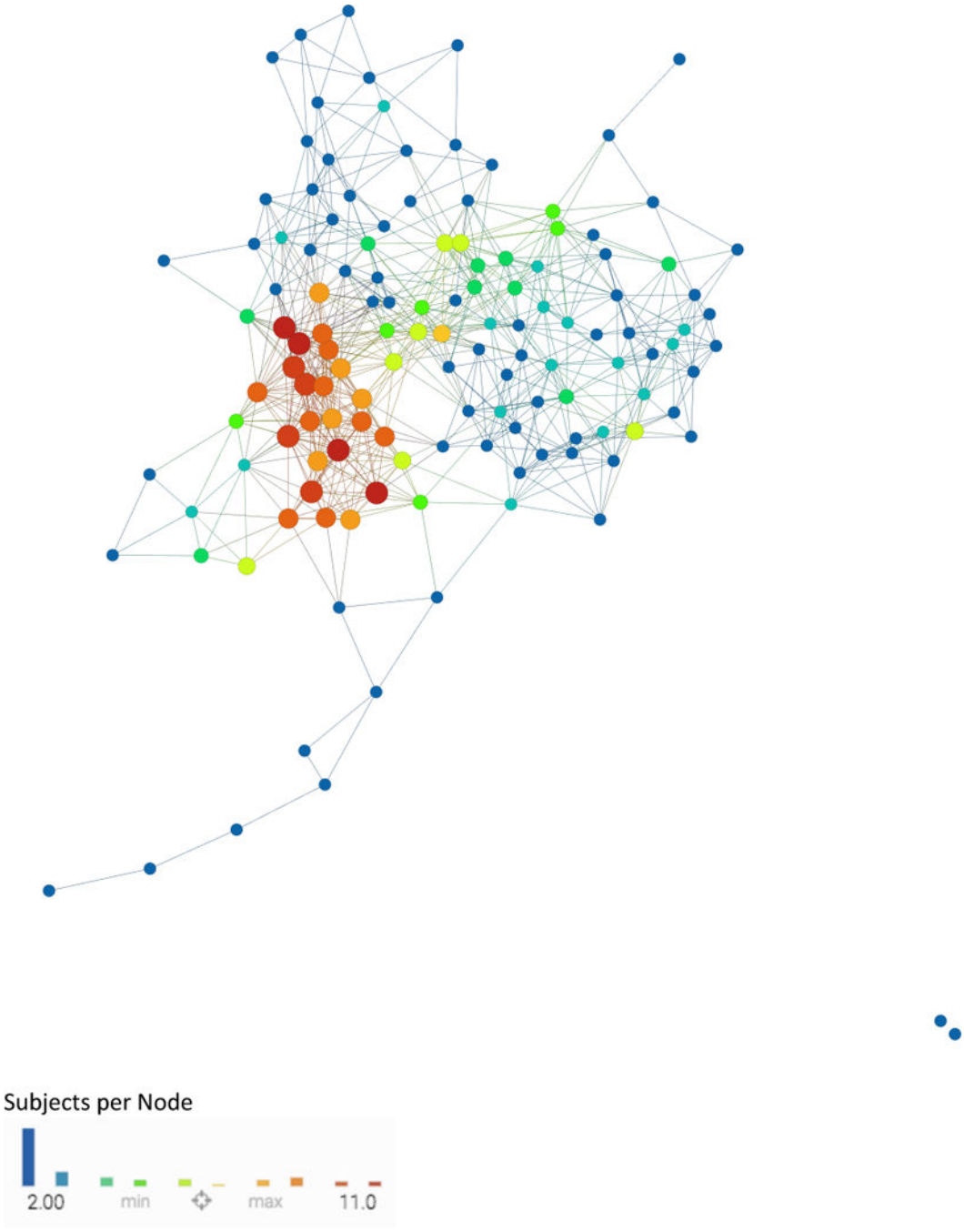

Figure 1. Combined network of morphological MRI, biomechanics, compositional MRI, and bone shape analysis

Each circle, or 'node', represents a subject or a collection of subjects. If two subjects are similar they are put together in the same node and if two nodes have enough in common they are connected by a line, or an 'edge.' The proximity of each node to another as well as the number of edges between two nodes represents the relative similarity of the subjects contained in each node. This network is color coded by subjects per node: Single subject nodes are expressed in blue and scale upwards towards red if a node has more subjects.

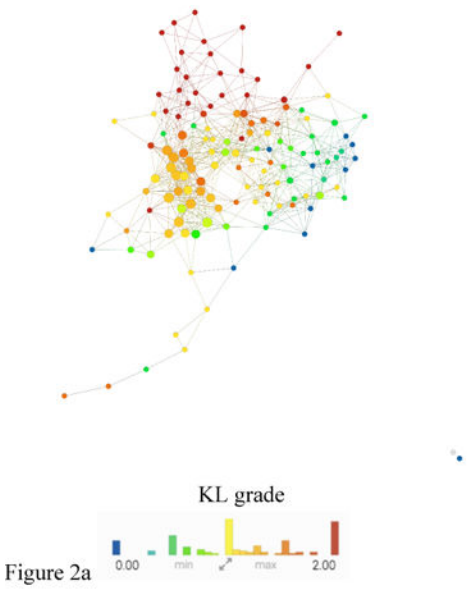

Figure 2a

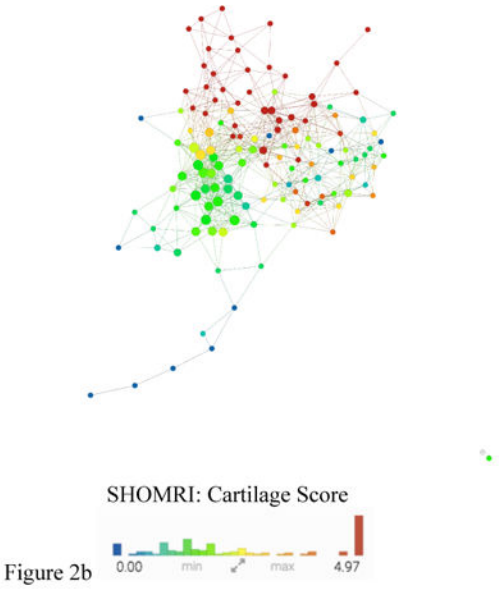

Figure 2b

Figure 2c

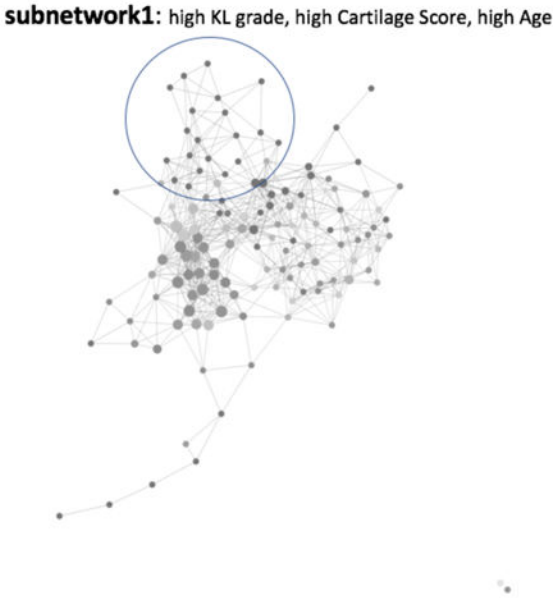

Figure 2d

Figure 2. Combined network of morphological MRI, biomechanics, compositional MRI, and bone shape analysis

a–c The same network is colored by KL grade, Total Cartilage Score, and Age. The combined network shows a pattern of standard signs of OA in the upper section of the network. **Figure 2d** shows severe patients appearing in the upper portion **subnetwork1** (circled with a blue line) and less severe in the lower portion based on the visual inspection of the combination of the three images **a-c**.

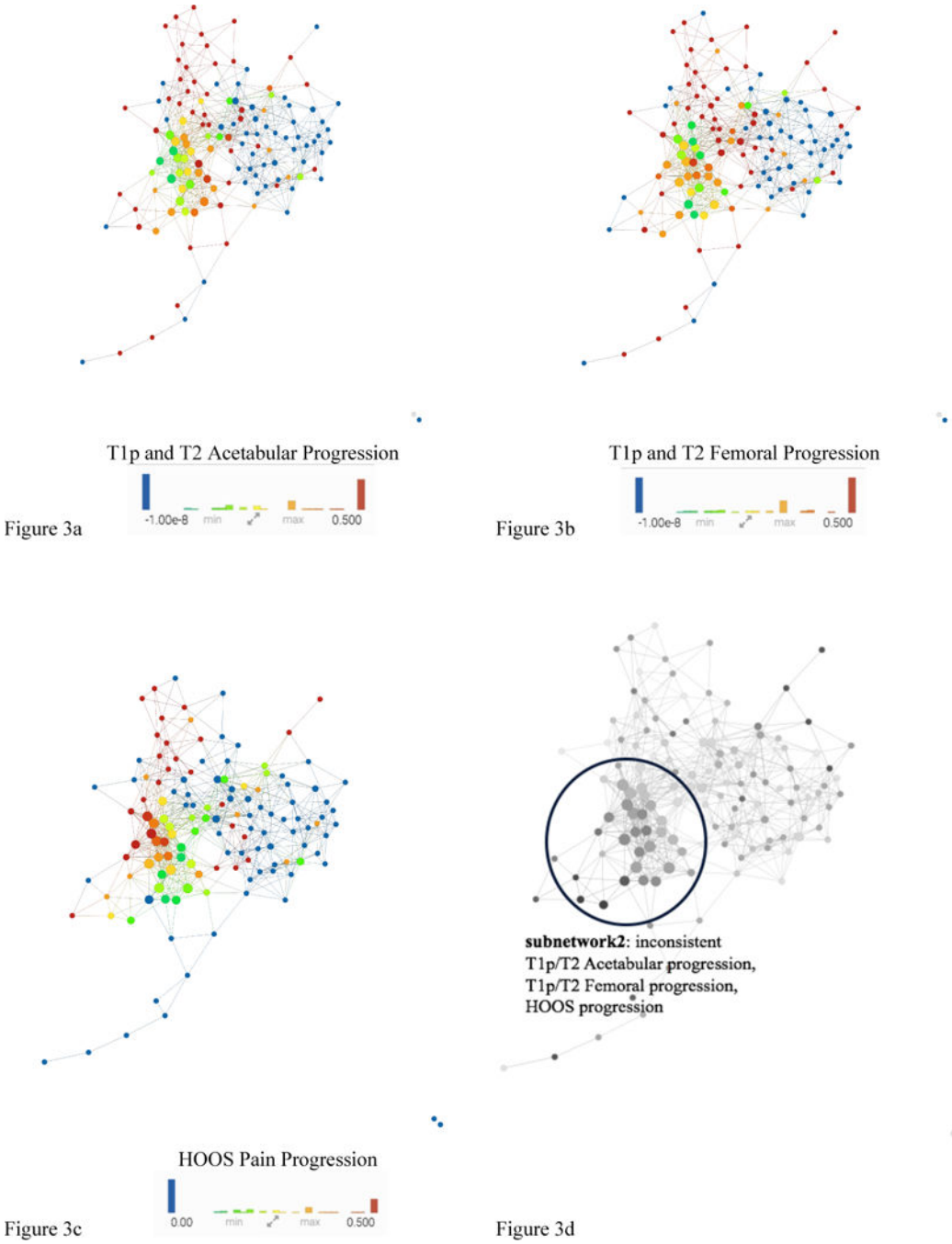

Figure 3. Combined network of morphological MRI, biomechanics, compositional MRI, and bone shape analysis

The same network is colored by **(A) $T_{1\rho}$ and T_2 Acetabular Progression**, **(B) $T_{1\rho}$ and T_2 Femoral, (C) HOOS Pain Progression**. Based on visual inspection of **a-c: Figure 3d** shows inconsistent progression patients appearing in the lower left portion **subnetwork2** (circled with a blue line) and consistent progression patients in the upper part of the network.

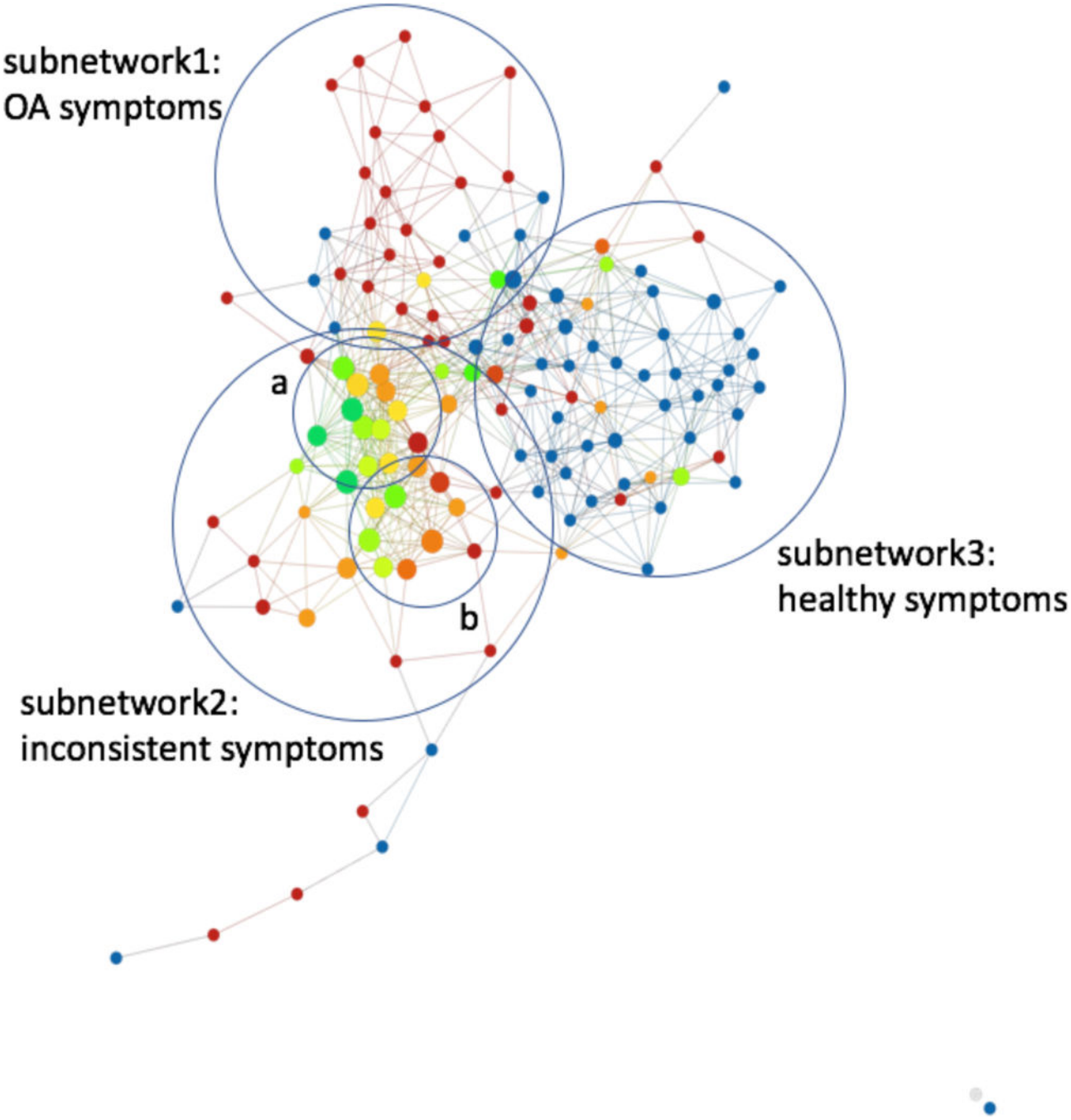

Figure 4. Final subdivision of the network

Subnetwork1 is made up of cohorts with high radiographic, morphological, compositional and symptomatic characteristics typical of OA. **Subnetwork3** is made up of cohorts with low radiographic, morphological, compositional, and biomechanical characteristics typical of a healthy cohort. **Subnetwork2** is made up of cohorts with typically lower knee kinetics and kinematics as well as **(a)**high symptomatic progression and **(b)**high compositional progression.

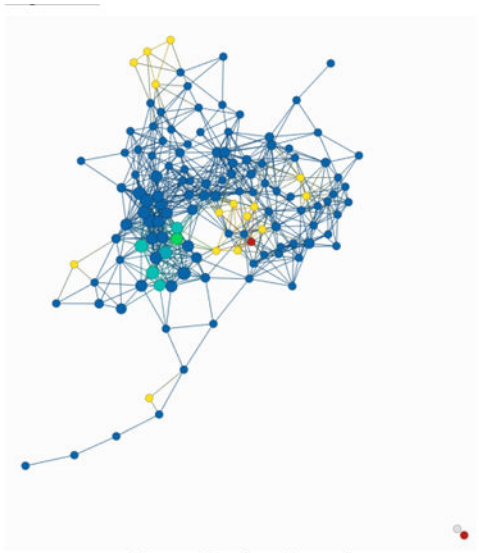

Figure 5a

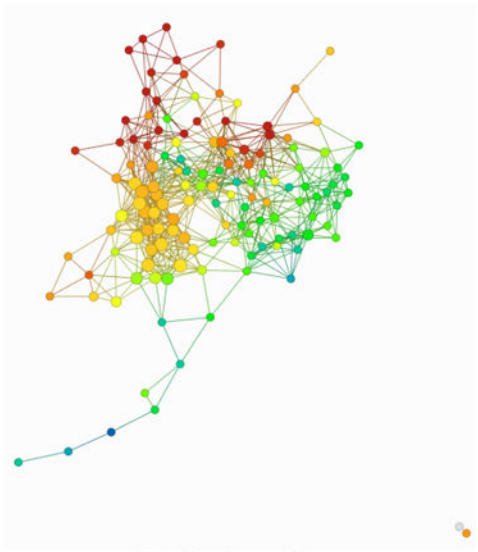

Figure 5b

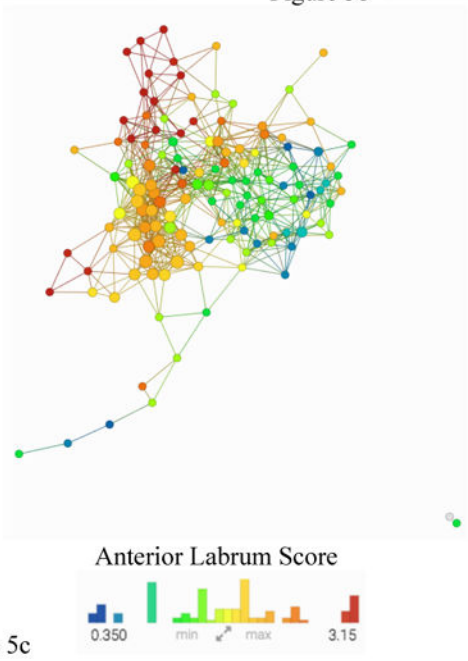

Figure 5c

Figure 5. Combined network of morphological MRI, biomechanics, compositional MRI, and bone shape analysis

The same network is colored **by (a) Group During Recruitment, (b)Total Labrum Score, (c) Anterior Labrum Score.** Based on visual inspection of **Figure 5a**: FAI patients are spread in both subnetwork1 and subnetwork3. **Figure 5b** and **Figure 5c** show similar coloring pattern to the KL colored network in Figure 2a.

Table 1

Demographics

Demographic characteristics (n=102)			
$T_{1\rho}/T_2$ Acetabular :	**Non Progressor (n=69)**	**Progressor (n=27)**	**P-value**
Age (avg±std)	43.1±13.4 years	47.0±14.1 years	0.25
Gender (F/M, %)	36 male (52%)	16 male (59%)	0.49
BMI (avg±std)	23.8±2.9 kg/m^2	24.1±3.5 kg/m^2	0.63
$T_{1\rho}/T_2$ Femoral :	**Non Progressor (n=72)**	**Progressor (n=28)**	**P-value**
Age (avg±std)	43.5±13.3 years	46.9±13.5 years	0.21
Gender (F/M, %)	37 male (52%)	15 male (54%)	0.90
BMI (avg±std)	23.7±2.9 kg/m^2	23.8±3.4 kg/m^2	0.94
HOOS Pain :	**Non Progressor (n=83)**	**Progressor (n=19)**	**P=value**
Age (avg±std)	42.6±13.3	50±13.8	**0.03**
Gender (F/M, %)	45 male (54%)	11 male (58%)	0.77
BMI (avg±std)	23.8±3.1 kg/m^2	23.8±2.7 kg/m^2	0.98

Table 2

a Subnetwork 1 compared to rest of cohort

ID	Variable	P-value	KS Score	Mean sub network1-rest
75	t0_SHOMRI_TotalCartilageScore	4.09E-10	0.7125	5.9
90	t0_SHOMRI_Total	2.12E-08	0.646428571	15.1
2	age	2.77E-07	0.598214286	13.4
41	t0_Coronal_SHOMRI_CartilageLesion.**FL**	3.10E-07	0.595535714	0.879
39	t0_Coronal_SHOMRI_CartilageLesion.**ASL**	3.66511E-06	0.547321429	0.829
42	t0_Coronal_SHOMRI_CartilageLesion.**FSL**	3.66511E-06	0.547321429	0.752
61	t0_Coronal_SHOMRI_ligamentumteres	6.09737E-06	0.535714286	1.01
63	t0_Sagittal_SHOMRI_CartilageLesion.**AA**	1.80376E-05	0.513392857	0.749
89	t0_SHOMRI_MiscTotal	3.50739E-05	0.498214286	1.34
65	t0_Sagittal_SHOMRI_CartilageLesion.**FA**	3.85077E-05	0.496428571	0.653
43	t0_Coronal_SHOMRI_CartilageLesion.**FSM**	0.000125043	0.467857143	0.689
138	t0_KneeKinetics_ExMImp2	0.000349274	0.458333333	22.7
81	t0_SHOMRI_TotalLabrumScore	0.000571268	0.430357143	4.3
44	t0_Coronal_SHOMRI_CartilageLesion.**FIM**	0.000619218	0.428571429	0.46
80	t0_Labrum_SHOMRI_ObliqueAxial.**PL**	0.000920998	0.416964286	0.809
9	KL GRADE	0.001256214	0.417888563	1.04
62	t0_Coronal_SHOMRI_SLL	0.001356221	0.40625	1.69
40	t0_Coronal_SHOMRI_CartilageLesion.**ASM**	0.001578859	0.402678571	0.516

b Subnetwork 2 compared to rest of cohort

ID	Variable	P-value	KS Score	Mean subnetwork2-rest
131	t0_KneeKinetics_PeakFlexM1	4.91E-08	0.613553114	0.25
133	t0_KneeKinetics_FlexMImp1	5.40E-07	0.56959707	−0.434
138	t0_KneeKinetics_ExMImp2	5.51162E-06	0.522893773	−31.4
41	t0_Coronal_SHOMRI_CartilageLesion.FL	1.34834E-05	0.486549708	−0.753
134	t0_KneeKinetics_FlexMImp2	1.63767E-05	0.5	−32.3
75	t0_SHOMRI_TotalCartilageScore	5.57266E-05	0.45497076	−3.87
137	t0_KneeKinetics_ExMImp1	6.68772E-05	0.470695971	−16.9
144	t0_KneeKinetics_PeakERM	0.000193187	0.445970696	0.0578
122	t0_KneeKinematics_PeakFlexAngle	0.000485635	0.423076923	5.38
127	t0_KneeKinematics_PeakAbduction	0.002467246	0.379120879	2.32
125	t0_KneeKinematics_FlexInitialContact	0.004691266	0.358974359	3.08
63	t0_Sagittal_SHOMRI_CartilageLesion.AA	0.008082509	0.330994152	−0.412
135	t0_KneeKinetics_PeakExM1	0.009223018	0.33974359	0.0798
65	t0_Sagittal_SHOMRI_CartilageLesion.FA	0.009223018	0.326315789	0.437
90	t0_SHOMRI_Total	0.011208835	0.320467836	−8.55
123	t0_KneeKinematics_SagExcursion	0.011952043	0.330586081	−2.3

b Subnetwork 2 compared to rest of cohort

ID	Variable	P-value	KS Score	Mean subnetwork2-rest
145	t0_HipKinematics_PeakFlex	0.013573266	0.326007326	−3.64